Heavy-ion stopping in solids: Energy transfer to the target or the dragging force due to the induced potential wake

Florian Grüner* and Friedhelm Bell
Department für Physik, Ludwig-Maximilians-Universität München, Am Coulombwall 6, D-85748 Garching, Germany
(Received 1 April 2005; published 31 August 2005)

There are two different approaches for describing the slowing down of charged particles in solids, commonly used in a separate way. Either one treats the energy transfer to the target or considers the dragging force due to the induced potential ("wake"). We herewith present a classical many-body calculation which intrinsically allows simultaneously both descriptions. For the first time, we can follow in detail the development of the stopping power, the projectile's charge and excitation state, as well as the formation of the wake, for ions entering into a solid. We further show that in nonequilibrium, stopping the development of the wake contributes much stronger to the change in stopping power than one could expect from the corresponding change of the projectile's charge or excitation state. This is exemplified by the explanation of an experimentally observed surface enhancement in the stopping power, which sheds new light on analysis tools with single atomic depth resolution. We underline our findings by simulating also anti-Ni ions, which are found to form a pressure wave in contrast to trailing wakes in the case of Ni ions.

DOI: 10.1103/PhysRevA.72.024902 PACS number(s): 34.50.Bw, 25.43.+t, 34.50.Fa, 61.85.+p

It is well known that the stopping power of swift charged particles in a solid can be described in two different ways: either by the probability for energy transfer to the medium, such as target excitation, ionization, and charge exchange, or by the electric field set up by induced charges acting as a dragging force on the particle. In his famous 1948 treatise "The penetration of atomic particles through matter" [1], Bohr showed for the first time that the strength of the electric field may simply be estimated by calculating the electric charge accumulated in the "wake" of the particle: "The mechanism of stopping of a particle passing through matter may be further elucidated by a direct estimate of the electric field which originates from the polarization of the medium and which acts as a kind of brake on the penetrating particle." An especially fruitful development of these ideas was the description of wake phenomena by the macroscopic polarization of the electron gas and its application to the stopping of heavy particles [2]. Since the basic excitation modes of an electron gas are either single particle or collective, i.e., plasmon excitations, especially the latter give rise to wakes with periodic electron density fluctuations behind the swift particle [3]. While such a dielectric formulation (DF) of ion stopping treats the medium in a global way, a microscopic treatment of the wake—as was the original idea of Bohr—and an extension of his first rough estimate of the stopping power to a more rigorous result seems to be lacking until today. Modern heavy-ion energy-loss theories [4] use the alternative route, i.e., they calculate in essence the probability for energy transfer to a single target atom. As single-atom theories, they do not follow the spatial development of the electron wake in a solid in order to specify quantitatively the change of the electron density induced by the projectile.

It is the aim of this paper to study wake formation by the ionization and excitation of individual atoms in a solid followed by scattering of these electrons on the projectile as well as on neighboring atoms, resulting in the final electron rearrangement in the form of a wake. For that we have extended the well known n-body classical trajectory Monte Carlo (nCTMC) method [5] to its applicability for the interaction of swift ions with atoms in a solid as described in the following section. The only other attempt in this direction known to us is the determination of the nuclear-track potential in insulators by Schiwietz and Xiao [6]. These authors have calculated, with a *single*-atom CTMC code, the potential induced by charges kept *fixed* at rest in the wake of a fast heavy ion traversing an insulator.

In contrast to earlier codes [5], in our nN-CTMC version, the ion interacts *simultaneously* with N target atoms each carrying n active electrons [7]. The Coulomb interaction of $N=16$ atoms with up to $n=6$ electrons has been followed on a time scale of 10^{-21} s. The use of smaller N's has shown that $N=16$ is sufficient to get N-independent results. At each time step, all Coulomb forces acting upon all particles are determined and Newton's law is applied for calculating the slowing down of the projectile nucleus as well as the classical trajectories of all electrons and target nuclei. The charge state of the projectile is simply determined by the number of all such electrons with a negative total energy in the projectile frame. We note that nN-CTMC does not need cross sections as input parameter, but delivers, if wanted, cross sections as a possible output. As usual, electron-electron interaction within a target atom is neglected, since a classical atom is unstable against autoionization. In the following, we choose as an example the wake formation by 1 MeV/u Ni ions in solid carbon [8], a typical case in the classical regime, where the distance of closest approach between the projectile and an electron is considerably larger than the electron wavelength in the rest frame of the projectile. The carbon atom is described by $n=6$ active electrons, whereas to the highly stripped Ni ion—in equilibrium the mean charge is $\langle Q\rangle = 17.6$ [8]—a fixed core-charge $Q_{\mathrm{core}}=22$ is assigned, which

*Electronic address: florian.gruener@physik.uni-muenchen.de

means that for a dressed ion with $Q=13$ the number of active electrons is 9. The introduction of a core charge has become necessary to restrict the number of active electrons in order to keep computation time realistic. We emphasize that, apart from the choice of the core charge, the simulation is free from any adjustable parameter; the only input parameters are the electron binding energies (orbital velocities are obtained via the virial theorem) and the occupation numbers. These initial conditions can easily be obtained for every projectile/target combination from single configuration Hartree-Fock calculations for atoms or ions.

Figure 1(a) shows the development of the mean charge $\langle Q(x)\rangle$ for a 1 MeV/u Ni ion in C as a function of the penetration depth x for initial charges $Q_{\mathrm{in}}=13$, 17, and 22. The mean equilibrium charge $\langle Q(x)_{\mathrm{eq}}\rangle=17.3$ compares favorably with the experimental value of 17.6 [8]. In Fig. 1(b), the corresponding stopping powers $\langle S(x)\rangle$ are plotted and the calculated equilibrium value $S^{\mathrm{eq}}_{\mathrm{sim}}=7.78$ keV/nm agrees well with the experimental $S^{\mathrm{eq}}_{\mathrm{expt}}=8.07$ keV/nm [8]. We strongly emphasize that the stopping power $S(x)\equiv dE/dx=\mathbf{v}\cdot\mathbf{F}(x)/v$ is given at any penetration depth x by the self-retarding Coulomb force $\mathbf{F}$ exerted from all charges on the projectile ion core, that is,

$$\mathbf{F}(x)=Q_c\sum_i Q_i(\mathbf{r}_i(x))\mathbf{r}_i(x)/[r_i(x)]^3, \tag{1}$$

where the summation i runs over all charges $Q_i(\mathbf{r}_i)$ except the ion core charge, $\mathbf{r}_i$ are the distances of these charges from the ion core, and $\mathbf{v}$ is the projectile velocity. Thus, variations of S as a function of x result merely from different spatial distributions of the $Q_i(\mathbf{r}_i(x))$. The difficulty in calculating $S(x)$ is thus transferred to obtain $Q_i(\mathbf{r}_i(x))$. We mention that in DF the $Q_i(\mathbf{r}_i)$ are calculated via the momentum (k) and frequency (ω) -dependent dielectric function $\epsilon(k,\omega)$, which specifies typically the linear response of the medium [3] in a global way, that is, not in the microscopic picture which also entails local processes such as charge exchange as presented here. While a formulation of S like that of Eq. (1) is always true, doubts may arise as to whether calculations of the energy transfer probabilities, which, at least in principle, could also generate $Q_i(\mathbf{r}_i(x))$, explicitly entail wake formation.

Figure 2 shows the ratio $\rho_i(r,z)/\rho_0$ of the induced and undisturbed charge density, where r is the distance perpendicular and z parallel to the ion trajectory taken in the ion frame. The undisturbed electron density $\rho_0=$const evidently does not contribute to the stopping power S.

Both $\rho_i(r,z)$ and ρ_0 have been obtained by taking "snapshots" of the electron positions for a large number of impinging ions at certain positions inside the target as given below. In DF one has $\rho_{\mathrm{ind}}(k,\omega)=\rho(k,\omega)(1/\epsilon(k,\omega)-1)$, where $\rho_{\mathrm{ind}}(k,\omega)$ and $\rho(k,\omega)$ are the Fourier transforms of the induced and ion charge density, respectively [3]. We also want to point out that our wake densities are the result of many *simultaneously* scattering electrons, which one may not get by just adding independent trajectories obtained from single-atom descriptions. It was found that polarized bound target electrons contribute only marginally to stopping, as their contribution to the enhanced wake density behind the projectile is just 10%. Figure 2 (top) is representative of an average wake in a 25-nm-thick carbon foil, where the snapshots have been averaged over all depths. Inspection of Fig. 1(b) reveals, however, that $\langle S(x)\rangle$ shows a pronounced peak at a penetration depth of about 0.6 nm for all three initial charge states. Thus, Fig. 2 (bottom) shows, for $Q_{\mathrm{in}}=22$, $\rho_i(r,z)/\rho_0$ at a depth of 0.6 nm. Pronounced differences of the wakes in Fig. 2 (top and bottom) are observed. Apparently, a dwell time of about 4×10^{-17} s, corresponding to a penetration depth $x=0.6$ nm, is too short to develop the steady-state wake of Fig. 2 (top), where the electron density is stretched further back from the projectile. The more intense charge

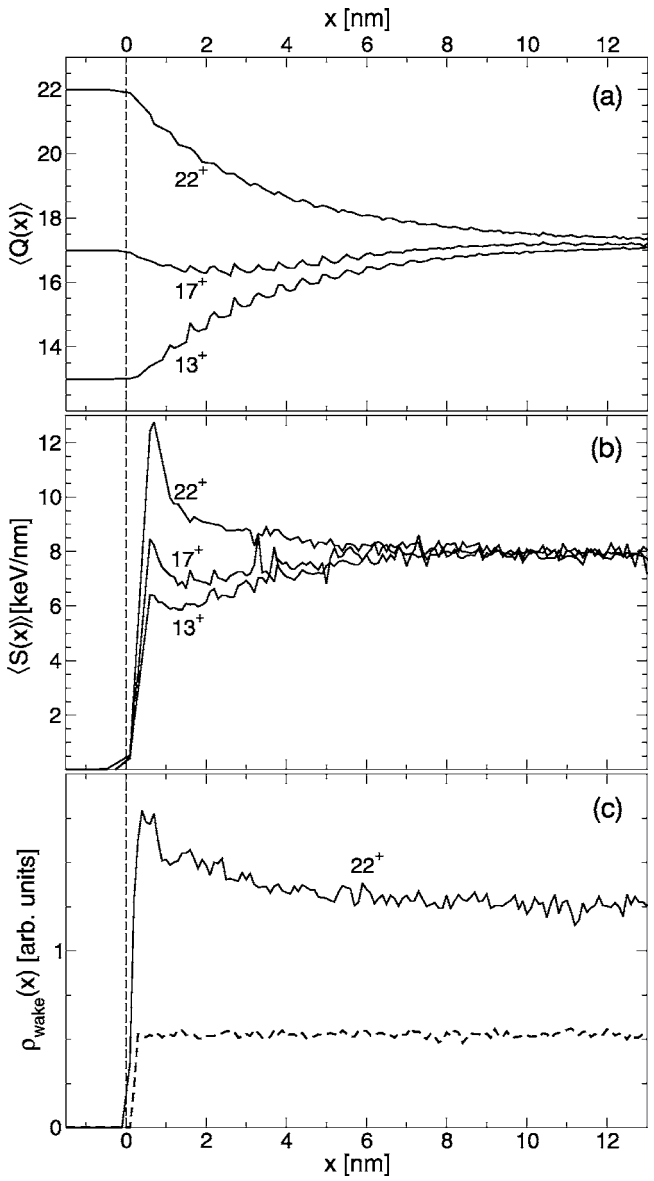

FIG. 1. Mean charge states (a) and corresponding stopping powers (b) of 1 MeV/u Ni ions in C vs penetration depth x for initial charge states $Q_{\mathrm{in}}=13$, 17, and 22. All three cases show clear surface peaks in $\langle S(x)\rangle$, despite only small changes in $\langle Q(x)\rangle$. (c) Wake density around 0.2 nm behind the projectile as a function of penetration depth x (solid line) compared to the undisturbed case (broken line) for $Q_{\mathrm{in}}=22$. One can see a qualitative correlation with the corresponding stopping power $S(x)$.

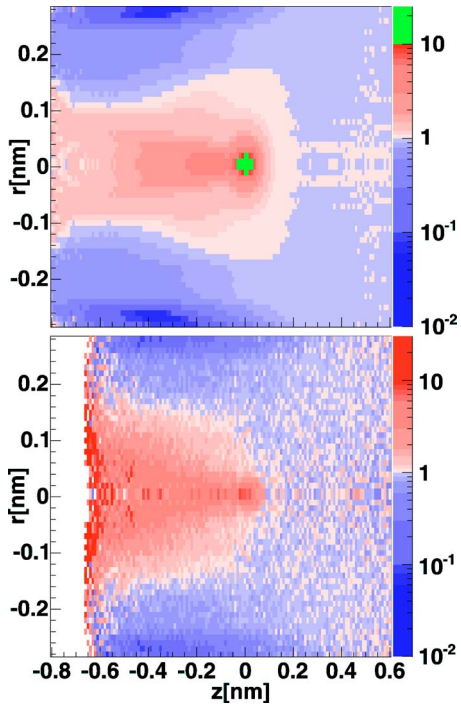

FIG. 2. (Color online) Ratio $R=\rho_i(r,z)/\rho_0$ of induced and undisturbed charge density, averaged over all depths x (top) and for $x=0.6$ nm (bottom) for $Q_{\mathrm{in}}=22$, relative to ion core in cylinder coordinates ($R>1$, $R<1$). The highest density (region in the top plot) is formed by captured electrons, which are not yet present for $x=0.6$ nm. The bottom wake is much more extended, explaining the surface stopping peak in Fig. 1. Overall there is charge conservation within a few percent.

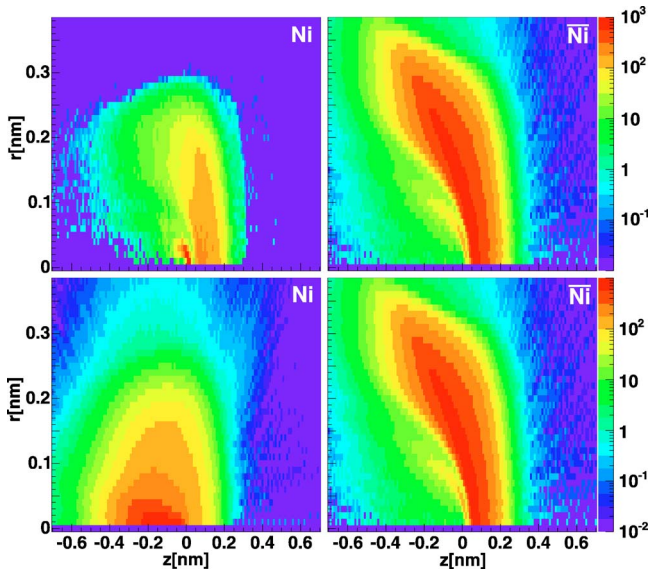

FIG. 3. (Color online) Instantaneous ionization locations, relative to ion core, for Ni (top left) and anti-Ni (top right), showing that most ionization events take place in front of the projectile, and corresponding spatial distribution of *free* electrons for Ni (bottom left) and anti-Ni (bottom right), having started from the ionization locations and finally forming the dragging wake (Ni) or pressure wave (anti-Ni). All plots are normalized to the same maximum value of 1000 in arbitrary units.

density behind the projectile compared to the steady-state wake is correlated directly with the enhanced stopping power peak at 0.6 nm, as indicated in Fig. 1(c), where the wake density around 0.2 nm behind the projectile is plotted against penetration depth x.

In the case of $Q_{\mathrm{in}}=22$, for instance, one may extrapolate the behavior of $S(x)$ underneath the peak toward the surface, thus getting a stopping without the surface peak. The resulting change in $\langle S(x)\rangle$ amounts then to 2% only and can very well be explained by the small change of the mean charge and/or excitation state of the projectile near the surface. However, the surface peak means a change in stopping of about 25%, more than an order of magnitude larger. This finding means that the *dynamic* rearrangement of electrons behind the projectile changes the stopping power by far more than any change of the charge or excitation state of the projectile alone. We are not aware that in the context of stopping theories such significant influences of wake formation have been discussed before [2,9]. Since the collective excitation process of the electron gas close to the surface is dominated by the generation of surface plasmons with energies smaller than the bulk plasmons, one would expect even a decrease in stopping power [9]. But we also note that in recent work about high-resolution elastic recoil detection (HERD) a strong enhancement of stopping power for 0.47 MeV/u I ions in highly oriented pyrolytic graphite (HOPG) up to the third layer as compared to tabulated values for bulk stopping has been observed [10], which seems to confirm our calculation. We also mention that difficulties in the reconstruction of the depth profile of the first monolayers in graphite as observed by Neumaier *et al.* [11], which had led to a discussion of possible clustering of carbon in the first layers, may be resolved if the surface peak above is taken into account. In high-resolution Rutherford backscattering (HRBS), Srivastava *et al.* [12] observed for 0.07 MeV/u N on HOPG a strong asymmetry in energy straggling for the uppermost layers—toward higher-energy losses—which could also be explained by the surface wake.

The findings above raise the important question about wake formation and its development. One may first ask from where the wake electrons originate. In Fig. 3 (top), the instantaneous ionization locations, defined as the places where the total electron energies in lab frame turn from negative values (bound electron) to positive ones (free electron), are plotted relative to the projectile position.

Clearly, these locations form a kind of bow wave [3], indicating that the high charge of the impinging Ni ion generates in essence ionization events in *front* of it. The corresponding electrons with velocities of less than an atomic unit in the lab frame form a kind of headwind with velocities of the projectile velocity in the ion frame. Scattered at the projectile they are focused at locations behind the projectile. We note that these ideas are very similar to the electron wind model developed by Steuer *et al.* [13] to explain the stopping power of nitrogen molecules in carbon foils. But we also state that this picture of wake formation is quite different from Bohr's original idea. There, the more or less "instantaneous" ionization locations are *behind* the projectile and

form, combined with rather *small* electron displacements, the wake. In contrast, in our case strong ionization takes place essentially *in front* of the projectile and thus demands rather *long* transportation distances for wake formation. It is readily seen from Fig. 3 that on the average the path length for electrons from the bow wave to the trailing wake is longer than 0.6 nm, which means that electrons as fast as the projectile do not have enough time to reach the final trailing wake position, explaining the not yet developed wake at a penetration depth of 0.6 nm. For a more detailed understanding of wake formation, it is worthwhile to look at the ionization locations corresponding to anti-Ni ions, which turned out to be approximately the same as for Ni ions, while Fig. 3 (bottom) shows a completely different "antiwake." Thus, while free electrons are similarly produced, different wakes arise between particles and antiparticles, clearly showing that wake formation is due to scattering on the projectile. This finding is also interesting in another aspect, the so-called Barkas effect [14], which is the difference in particle and antiparticle stopping. For heavy ions, there seem to be two opposite influences at work [15]. On one hand, target polarization increases ionization, and thus enhances S for particles compared to antiparticles. On the other hand, captured electrons in the case of Ni screen the Coulomb interaction and thus decrease S compared to anti-Ni, which cannot capture any electrons. We found that the equilibrium stopping of anti-Ni is *larger* by 4% than in the case of Ni, for which there is a dragging force due to the wake *behind* the Ni ion but a pressure force due to the bow wave *in front* of the anti-Ni.

In conclusion, by using a simulation where all physics is given exhaustively by the pure Coulomb's law applied to a classical many-body system, we have studied in detail the formation of the wake induced by a swift heavy ion in a solid. In contrast to Bohr's original concept, in our case of Ni ion stopping the electrons forming the wake are definitely generated in ionization processes which mostly occur in front of the ion. Thus, the wake formation results in the subsequent scattering of these freed electrons on the projectile. This kind of wake formation generates "surface wakes" not been predicted by either theories which describe stopping by energy transfer probabilities or dielectric formulations, but apparantly confirmed by recent high-resolution energy-loss experiments.

The key message is that calculations which only treat energy transfer to a target atom fail in describing the entire picture of stopping which, according to our results, includes wake formation, especially around the surface. To the best of our knowledge, we are the first to show that experimentally found stopping enhancements around the surface cannot be attributed to the almost negligible change in charge and excitation state, but only a change in the target, namely the development of a wake. One can go even further: stopping happens if and only if there is a redistribution of target electrons, therefore any stopping is not just a simple energy transfer but a much more complex process.

This work was supported by the Deutsche Forschungsgemeinschaft (DFG) under Contract No. GR2120/1-1.

[1] N. Bohr, K. Dan. Vidensk. Selsk. Mat. Fys. Medd. **18**, No. 8 (1948).

[2] J. Lindhard, K. Dan. Vidensk. Selsk. Mat. Fys. Medd. **28**, No. 8 (1954); J. Neufeld and R. H. Ritchie, Phys. Rev. **98**, 1632 (1955); **99**, 1125 (1955); R. H. Ritchie, W. Brandt, and P. M. Echenique, Phys. Rev. B **14**, 4808 (1976); P. M. Echenique, F. J. Garcia de Abajo, V. H. Ponce, and M. E. Uranga, Nucl. Instrum. Methods Phys. Res. B **96**, 583 (1995).

[3] P. M. Echenique, R. H. Ritchie, and W. Brandt, Phys. Rev. B **20**, 2567 (1979).

[4] P. Sigmund and A. Schinner, Nucl. Instrum. Methods Phys. Res. B **195**, 64 (2002); P. L. Grande and G. Schiwietz, *ibid.* **195**, 55 (2002); G. Maynard, G. Zwicknagel, C. Deutsch, and K. Katsonic, Phys. Rev. A **63**, 052903 (2001).

[5] R. E. Olson, J. Ullrich, and H. Schmidt-Böcking, Phys. Rev. A **39**, 5572 (1989); R. E. Olson, Radiat. Eff. Defects Solids **110**, 1 (1989); P. L. Grande and G. Schiwietz, J. Phys. B **28**, 425 (1995).

[6] G. Schiwietz and G. Xiao, Nucl. Instrum. Methods Phys. Res. B **107**, 113 (1996).

[7] F. Grüner, F. Bell, W. Assmann, and M. Schubert, Phys. Rev. Lett. (to be published).

[8] C. M. Frey, G. Dollinger, A. Bermaier, T. Faestermann, and P. Maier-Komor, Nucl. Instrum. Methods Phys. Res. B **107**, 31 (1996).

[9] R. H. Ritchie, Phys. Rev. **106**, 874 (1957); C. C. Sung and R. H. Ritchie, J. Phys. C **14**, 2409 (1981); P. Sigmund, Nucl. Instrum. Methods Phys. Res. B **95**, 477 (1995); S. B. Trickey, J. Z. Wu, and J. R. Sabin, *ibid.* **93**, 186 (1994).

[10] G. Dollinger, C. M. Frey, A. Bergmaier, and T. Faestermann, Europhys. Lett. **42**, 25 (1998).

[11] P. Neumaier, G. Dollinger, A. Bergmaier, I. Genchev, L. Görgens, R. Fischer, C. Ronning, and H. Hofsäss, Nucl. Instrum. Methods Phys. Res. B **183**, 48 (2001).

[12] S. K. Srivastava, D. Plachke, A. Szökefalvi-Nagy, J. Major, and H. D. Carstanjen, Nucl. Instrum. Methods Phys. Res. B **219-220**, 364 (2004).

[13] M. F. Steuer, D. S. Gemmell, E. P. Kanter, E. A. Johnson, and B. J. Zabransky, IEEE Trans. Nucl. Sci. **NS-30**, 1069 (1983).

[14] W. H. Barkas, W. Birnbaum, and F. M. Smith, Phys. Rev. **101**, 778 (1956).

[15] P. Sigmund and A. Schinner, Nucl. Instrum. Methods Phys. Res. B **212**, 110 (2003).